BULLETIN OF THE POLISH ACADEMY OF SCIENCES
TECHNICAL SCIENCES, Vol. 69(6), 2021, Article number: e139790
DOI: 10.24425/bpasts.2021.139790

Model-based initial residual unbalance identification for rotating machines in one and two planes using an iterative inverse approach

Satish BASTAKOTI[1], Tuhin CHOUDHURY[1*], Risto VIITALA[2], Emil KURVINEN[1], and Jussi SOPANEN[1]

[1] Department of Mechanical Engineering, School of Energy Systems, Lappeenranta-Lahti University of Technology LUT, 53850 Lappeenranta, Finland

[2] Department of Mechanical Engineering, School of Engineering, Aalto University, 00076 Espoo, Finland

Abstract. To achieve acceptable dynamical behavior for large rotating machines operating at subcritical speeds, the balancing quality check at the planned service speed in the installation location is often demanded for machines such as turbo-generators or high-speed machines. While most studies investigate the balancing quality at critical speeds, only a few studies have investigated this aspect using numerical methods at operational speed. This study proposes a novel, model-based method for inversely estimating initial residual unbalance in one and two planes after initial grade balancing for large flexible rotors operating at the service speeds. The method utilizes vibration measurements from two planes in any single direction, combined with a finite element model of the rotor to inversely determine the residual unbalance in one and two planes. This method can be practically used to determine the initial and residual unbalance after the balancing process, and further it can be used for condition-based monitoring of the unbalance state of the rotor.

Key words: flexible rotor; inverse approach; onsite-balancing; residual unbalance; single and double plane.

1. INTRODUCTION

Mass unbalance is the most significant fault [1] occurring in rotating machines that leads to excessive vibration and undesired load on the bearings, eventually leading to degradation of bearings. Such unbalance may occur due to inhomogeneous material properties, limitations in manufacturing and assembly or component failures or cracks in the rotating part. During initial functional testing, the unbalance (out of balance) masses are identified by using balancing techniques such as Influence Coefficient Method (ICM) [2–6], modal balancing method [7–10] and unified balancing method [11]. Accordingly, counterbalancing masses are added in correction planes to mitigate vibration to predefined limit [12]. Depending on the application, balancing classes, e.g. G1.6, allow certain amount (g · m/kg of the rotor) of residual unbalance in the rotor at operational speed due to limitation in manufacturing, part tolerance, cost or assembly.

In many cases, the initial balancing is performed on standalone rotors in balancing machines and the estimation of onsite balancing quality at operational speed is often required to guarantee the operation. The remaining residual unbalance is randomly distributed along the length of the shaft and its magnitude and phase are unknown. However, a resultant residual unbalance (a resultant vector of all the continuous, randomly distributed unbalance) can be considered to be located along the length of the rotor at a single plane or two planes. For onsite balancing, the resultant unbalance or unbalances have to be determined at the single or multiple available balancing planes.

While the traditional balancing methods such as influence coefficient method (ICM) [6] or modal balancing method [8] require multiple trial runs with trail masses, the model-based approach utilizes a simulation model in combination with measured signal to directly identify the unbalance mass, axial location, and phase. Typically, such methods require two sets of measurement: a measurement for the fault system and a baseline measurement of the ideal system [13]. Hence, they are suitable for condition monitoring of machines under actual operating conditions [14]. In a study where the vibration signature between an ideal and a faulty system are compared, Markert *et al.* [14] proposed that the change in vibration can be attributed to an equivalent load instead of the change in unbalance. The location of the maximum load gives the unbalance location. A comparison of the equivalent load with the theoretical unbalance forces yields the unbalance parameters. Many studies have proposed a similar method where the equivalent load is combined with modal expansion and an optimization algorithm such as least squares for identifying the unbalance parameters [14–17]. Other studies have utilized residual mapping techniques [18, 19], M-estimator [20], extended [1] and augmented [21] Kalman filters, and machine learning techniques [22–24] for estimating unbalance.

Some researchers such as Sinha *et al.* [25, 26], Edwards *et al.* [27], and Lees *et al.* [28, 29] also proposed methods that can identify the unbalance parameters with a single measure-

*e-mail: Tuhin.Choudhury@lut.fi

Manuscript submitted 2021-03-16, revised 2021-11-22, initially accepted for publication 2021-12-01, published in December 2021

ment, which makes them suitable for identifying the initial unbalance at commissioning stages as well. In more recent years, Shamsah *et al.* [30] proposed a way for reducing the number of sensors for a given bearing location. Their study shows that a single sensor at 45° angle can replace both horizontal and vertical displacement sensors for estimated unbalance. In other studies [31, 32] this method of reduced sensors was combined with the single rundown method proposed in [25].

Recent studies have also focused on the onsite balancing of flexible rotors at the operational speed using model-based numerical counterparts of ICM [33] or modal balancing method [34]. For example, in the numerical ICM method, the coefficient matrices are determined numerically for identifying the unbalance [35] at pre-determined balancing planes.

For initial residual identification either at the resultant unbalance location or at the predetermined balancing planes, the baseline vibration is unavailable. The location of resultant residual unbalance is important for cases where, for example, there are multiple impellers or discs, and the goal is to determine which of the discs has the highest amount of fouling or accumulated dirt. On the other hand, such a method should also have the capability of estimating the unbalance magnitudes and phases at the balancing planes so that, after identification, there is a possibility for balancing as well. There is a requirement for a method which can identify the resultant residual unbalance location, as well as the unbalance parameters at the balancing planes.

Therefore, this study proposes a method of using a more direct approach to identify the resultant unbalance in a one or two random planes, as well as on the predetermined balancing planes using a single run, without the necessity of calculating coefficients. The numerical method uses an inverse iterative approach to directly determine the residual unbalance. The method requires a finite element (FE) model and measurements from two planes in any single direction to identify the residual unbalance in one and two planes. Using a single run of measured absolute displacement of the rotor at operational speed as a reference, the simulated signal from the model is iterated by varying the unbalance at the balancing planes until it matches the measured signal.

The test rotor under study is a guiding roll of a paper machine. This large flexible rotor has three sections, from which the tubular body in the middle mainly causes the unbalance of the rotor. The residual unbalance is distributed along the rotor that makes it an interesting case for this study. The test rotor has been initially balanced, and the objective is to identify the remaining residual unbalance at one and two planes. The single plane approach aims to identify the single resultant unbalance plane which represents the combined effect of all the distributed unbalance in the rotor. The two-plane approach aims to identify the residual unbalance in a combination of two planes along the rotor length for the best match and the results are compared with the values of the single plane. In case the balancing quality is acceptable, and the remaining residual unbalance is below the permissible limit, the identified residual unbalance can be integrated into the model to accurately replicate the dynamic behaviour of the machine in digital twin applications.

The proposed numerical iterative method can be further used for condition-based monitoring (CBM) of the unbalance state of the rotor using a digital twin approach similar to the numerical ICM [35] or modal balancing method [34] in the literature. The proposed model can be used to assess the unbalance state in real-time from the continuously updated measured displacements. This allows us to trace changes during the operation and identify issues at an early stage.

2. METHODS

The proposed method is applicable to flexible rotors operating at out of resonance speed. As per ISO 21940-12 [36], a rotor is flexible if the first flexural resonance speed is within 50% of the maximum service speed. The method uses a FE model that generates the unbalance response of the rotor-bearing-support system based on the input unbalance magnitude and phase. The system equations can be represented as follows

$$\mathbf{M}\ddot{\mathbf{x}}(t)+(\mathbf{C}+\omega\mathbf{G})\dot{\mathbf{x}}(t)+\mathbf{K}\mathbf{x}(t)=\mathbf{F}_v\sin\omega t+\mathbf{F}_h\cos\omega t, \quad (1)$$

where $\mathbf{M}$, $\mathbf{C}$, $\mathbf{K}$ and $\mathbf{G}$ are the mass, damping, stiffness and gyroscopic matrices respectively and ω is the rotational speed of the rotor. $\mathbf{F}_v$ and $\mathbf{F}_h$ are the vertical and horizontal components of the unbalance force as follows:

$$\mathbf{F}_v = me\omega^2\big[\sin(\omega t+\phi)\big], \quad (2)$$

$$\mathbf{F}_h = me\omega^2\big[\cos(\omega t+\phi)\big], \quad (3)$$

where m, e and ϕ represent the mass, eccentricity, and phase of the unbalance respectively. Now using a trial solution of the form

$$\mathbf{x}(t)=\mathbf{a}\sin\omega t+\mathbf{b}\cos\omega t, \quad (4)$$

the system displacements can be obtained. The coefficient vectors $\mathbf{a}$ and $\mathbf{b}$ can be solved for the harmonic excitation force as follows:

$$\begin{bmatrix}\mathbf{a}\\ \mathbf{b}\end{bmatrix}=\begin{bmatrix}\mathbf{K}-\mathbf{M}\omega^2 & -\omega(\mathbf{C}+\omega\mathbf{G})\\ \omega(\mathbf{C}+\omega\mathbf{G}) & \mathbf{K}-\mathbf{M}\omega^2\end{bmatrix}^{-1}\begin{bmatrix}\mathbf{F}_v\\ \mathbf{F}_h\end{bmatrix}. \quad (5)$$

Equation (5) can be simplified as follows:

$$\big[\mathbf{P}\big]=\big[\mathbf{A}\big]^{-1}u_n\omega^2\begin{bmatrix}\sin(\omega t+\phi)\\ \cos(\omega t+\phi)\end{bmatrix}, \quad (6)$$

where $\mathbf{P}$ represents the coefficient vector which is directly correlated to the displacements $\mathbf{x}$, $\mathbf{A}$ represents the combination of system matrices in equation (5), the force vectors $\mathbf{F}_v$ and $\mathbf{F}_h$ are expanded and u_n represents the unbalance magnitude at node n, comprising of the unbalance mass and eccentricity.

2.1. Inverse iterative approach

Using the above solution procedure, the 1X (once per revolution) response solution can be obtained at the desired nodal location (DOFs) from the model. Using this procedure in an iterative approach for a range of unbalance magnitude, node location

and phase, the response is compared in a loop with the measured data to identify the best matching unbalance parameters location at two planes. Figure 1 shows the overall process flow.

The single plane approach aims to identify the single resultant unbalance plane which represents the combined effect of all the distributed unbalance in the rotor. The two-plane approach aims to identify the residual unbalance in a combination of two planes along the rotor length for the best match and the results are compared with the values of the single plane. In both cases, the unbalance is identified by iteratively providing unbalance parameters in the simulation model and matching the numerically generated vibration to the measured signals. The one and two plane residual unbalances (either one can be chosen depending on the accuracy) will confirm the quality of the initial grade balancing. To further validate the identified residuals, known balancing masses are added both to the simulation model as well as the experimental rotor and the output vibration signals are compared.

If the remaining residual unbalance is unacceptable, using the two-plane approach, the residual unbalance can be identified in the two possible balancing planes for a rotor operating near the first critical speed. Once the resultant residual unbalance (magnitude and phase) is known at the balancing planes, field balancing can be done by adding or removing the balancing masses in those planes at correct phase locations to balance the rotor according to its balancing class [8, 9].

2.1.1. Single plane approach

The single plane approach is a very basic and simplistic method to approximately estimate the residual unbalance in a single plane. It serves as a validation tool that the measured system and simulated systems are in the right scale, i.e. the models are from the same machine and no large errors occurred during the measurements or while creating of a simulation model. For a flexible rotor operating at a speed where the operational deflection shape (ODS) is affected by the first critical speed, typi-

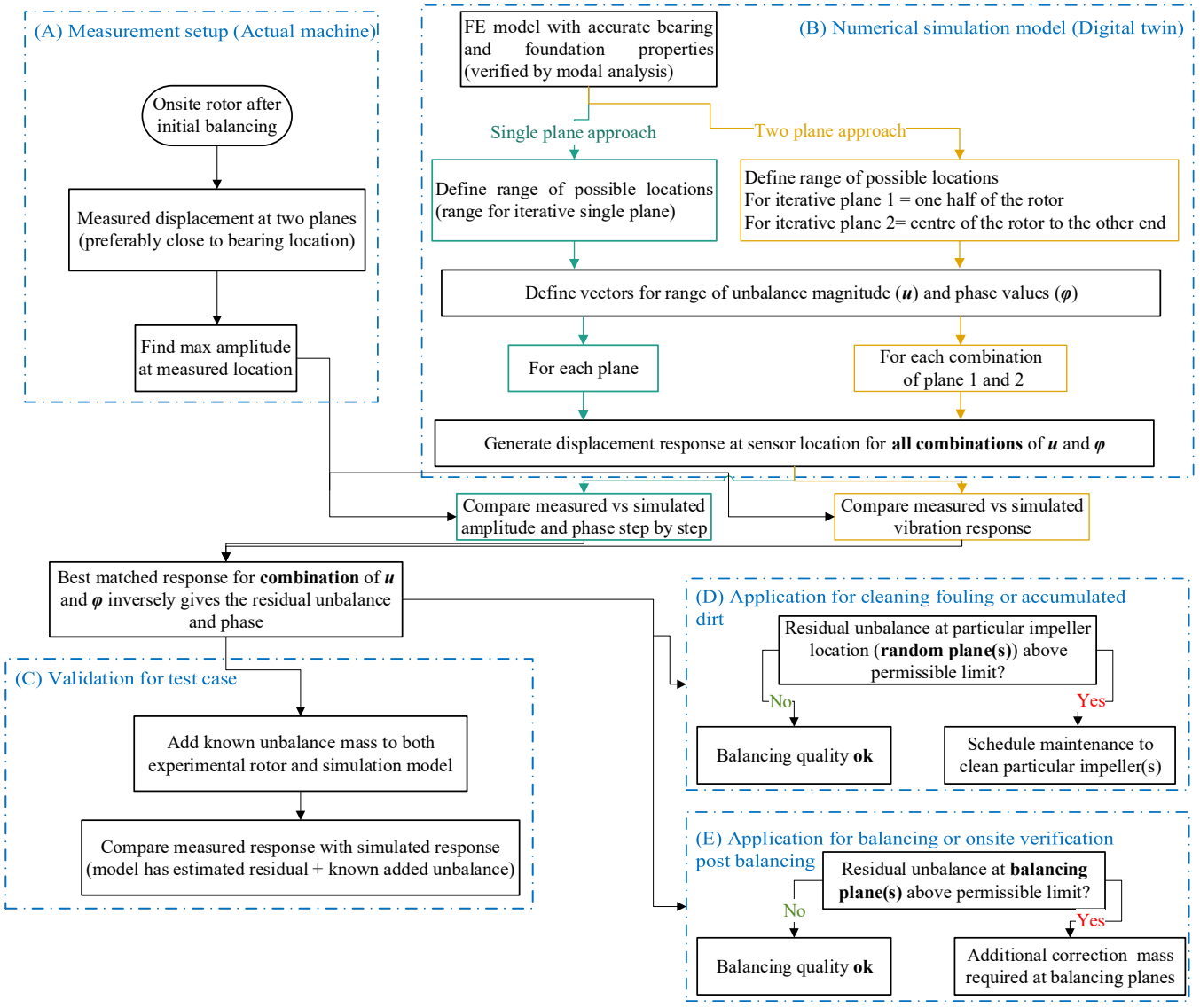

Fig. 1. Generalized process flow for the method proposed in this study

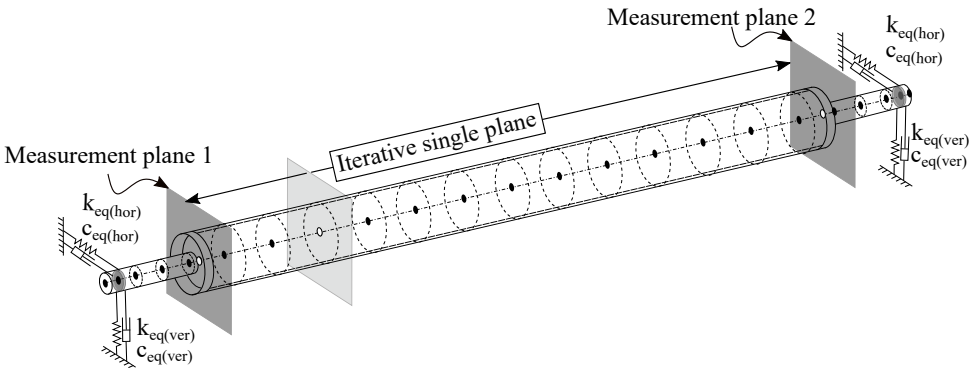

Fig. 2. Single plane iterative approach which can be used for a rough estimation of the resultant residual unbalance in the rotor

cally it is not possible to accurately estimate the residual unbalance and requires a minimum of two planes [8,9]. Theoretically, however, each of the residual unbalances in every single plane along the rotor plane can be combined together into a resultant vector of unbalance in a single plane. Figure 2 depicts a guiding roll of a paper machine. Variables k_{eq} and c_{eq} represent the equivalent stiffness and damping of the bearing and support in their respective directions. For such a rotor, the residual unbalance is most probably randomly distributed in the thin-walled, tubular section along the length of the rotor in multiple planes.

Therefore, to identify the resultant of all these random unbalances, a range of values can be considered at the iterative plane, which is at the first location on the left end of the tube. For these unbalance values, the responses can be obtained at measurement planes (closest possible planes to the bearings) and the amplitudes can be compared with those from the measured responses at the respective planes. Note that once the amplitude and location are known, the phase is iterated for the single plane residual to match the vibration signals from the model with the measured data.

The first loop of iteration is for the unbalance magnitude. Considering an increment of Δu for each iteration and an assumed maximum value of unbalance as $u_n^{\max}$, the i-th iteration of unbalance, u_n^i is:

$$u_n^i = u_n^{i-1} + \Delta u,\ 0 < u_n^i \leq u_n^{\max} \tag{7}$$

Equation (7) is carried out for each location or nodes of the model. This creates a second loop of iteration, adding the mathematical condition below to equation (7)

$$1 \leq n \leq n_{\text{total}} \tag{8}$$

where n_{total} is the total number of nodes. For the maximum displacement or amplitude value, the sine and cosine terms in equation (6) are unity and the response coefficients are directly proportional to the unbalance magnitude only and the effect of the unbalance phase is eliminated.

$$\left[\mathbf{P}\right] = \left[\mathbf{A}\right]^{-1} u_n \omega^2 . \tag{9}$$

Using the two iteration loops over equation (9), the displacement amplitude from the model can be matched with the amplitude from the 1X response of the measured displacement, where the iteration with minimum difference yields the location and unbalance magnitude.

$$\min(|\, x_{\max\,(\text{model})} - x_{\max\,(\text{meas})}\,|) \rightarrow \{u^i, n\}. \tag{10}$$

For single-plane unbalance, the phase correction is performed once the plane location and magnitude of unbalance is identified such that the simulation model generates the best match for amplitude in the measured coordinates. Since the maximum displacement is known, the phase of the unbalance is obtained simply by correcting the displacement signal phase in the model (α_{model}) to match the measured signals (α_{meas}).

$$\min(|\, \alpha_{\text{model}} - \alpha_{\text{meas}}\,|) \rightarrow \{\phi^i\}. \tag{11}$$

2.1.2. Two planes approach

In principle, the two planes approach is similar to the single plane approach discussed in section 2.1.1. One major difference is that instead of a single plane, two iterative planes are used here (Fig. 3). The first plane iterates (n_1) over locations from one end of the tube section to the centre, while the other plane (n_2) iterates over the remaining possible locations. Since the relative phase is of importance here, the unbalance magnitude and phase are iterated together for each location of the iterative plane.

$$\left.\begin{aligned} \{u_1\}_{n_1}^i &= \{u_1\}_{n_1}^{i-1} + \Delta u \\ \{\phi_1\}_{n_1}^i &= \{\phi_1\}_{n_1}^{i-1} + \Delta\phi \end{aligned}\right\} \begin{aligned} &0 < \{u_1\}_{n_1}^i \leq \{u_1\}_{n_1}^{\max}, \\ &0^\circ \leq \{\phi_1\}_{n_1}^i \leq 360^\circ, \\ &1 \leq n_1 < n_{\text{total}}/2, \end{aligned} \tag{12}$$

$$\left.\begin{aligned} \{u_2\}_{n_2}^i &= \{u_2\}_{n_2}^{i-1} + \Delta u \\ \{\phi_2\}_{n_2}^i &= \{\phi_2\}_{n_2}^{i-1} + \Delta\phi \end{aligned}\right\} \begin{aligned} &0 < \{u_2\}_{n_2}^i \leq \{u_2\}_{n_2}^{\max}, \\ &0^\circ \leq \{\phi_2\}_{n_2}^i \leq 360^\circ, \\ &n_{\text{total}}/2 \leq n_2 < n_{\text{total}}\,. \end{aligned} \tag{13}$$

Using these iterations together with a minimization of the vibration signals, the unbalance parameters can be identified for the two planes.

$$\min(|\, x(t)_{\text{model}} - x(t)_{\text{meas}}\,|) \rightarrow \{u^i, \phi^i, n\}_{1,2}\,. \tag{14}$$

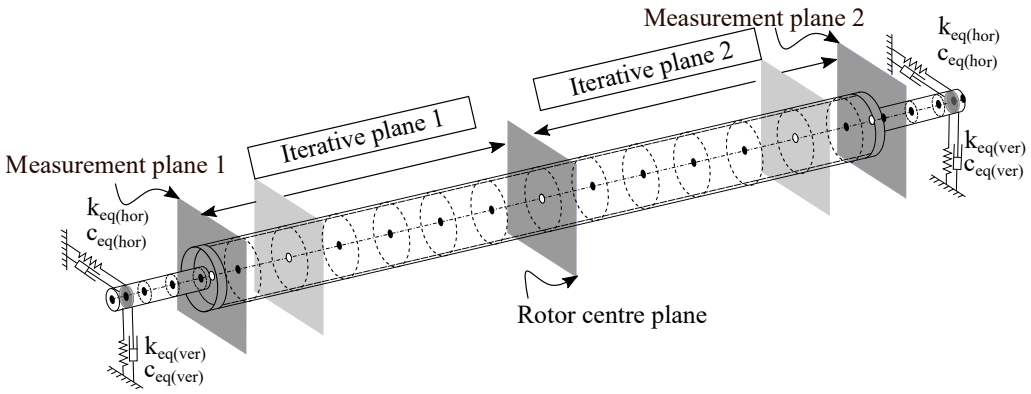

Fig. 3. Iterative approach with two planes for estimation of the resultant residual unbalance in the rotor

Since the residual unbalance is identified in two planes, their relative phase will affect the simulated responses at both measurement planes. Thus, two plane method can better represent the force distribution (compared to the single plane) and therefore yields better estimation [33], especially in case of flexible rotors as the resultant force in a single plane may generate larger dynamic bending in the rotor compared to actual distributed unbalance situation, and hence develop error to the residual unbalance.

2.2. Test case, measurement, and simulation model

To test the residual unbalance identifying algorithm, a guiding roll of a paper machine is studied which is a slender continuous tube with thin walls and hence a more evenly distributed mass system. The test rotor is flexible as the first resonance speed in a horizontal direction (1260 rpm) is only 30% above the operational speed and balancing speed (960 rpm). The rotor total length is five meters and it weighs 719 kg.

2.2.1. Measurement setup

Figures 4 and 5 show the test setup in which the guiding roll of a paper machine was studied. The test rotor was initially balanced by applying the ICM [37] with two balancing planes using the radial bearing force measurement as feedback. This means that the radial bearing forces were minimized during the balancing process and thus, the orbit of the rotor was nearly circular even though the foundation of the rotor was anisotropic. Table 1 lists the used balancing masses. Since the rotor was flexible and its balancing state changes due to dynamic bending, the balancing could be optimized only at a certain rotating frequency when ICM with two planes was used as a balancing method.

Suitable experimental data could be acquired to verify the proposed simulation-based method when four different unbalance cases were measured. In the first case, the balanced rotor was measured with some residual unbalance (as it is stated). In the following cases the unbalance is increased with additional masses which were attached only to the other end (NDE) of the rotor. The additional masses were approximately 100 g, 300 g and 500 g.

The center point movement of the rotor was measured from two different cross-sections along the rotor. The same cross-sections were measured as the ones observed in the simulation model. These cross-sections are illustrated in Fig. 6 as nodes 6 and 20. A four-point method [38] was used for measurement

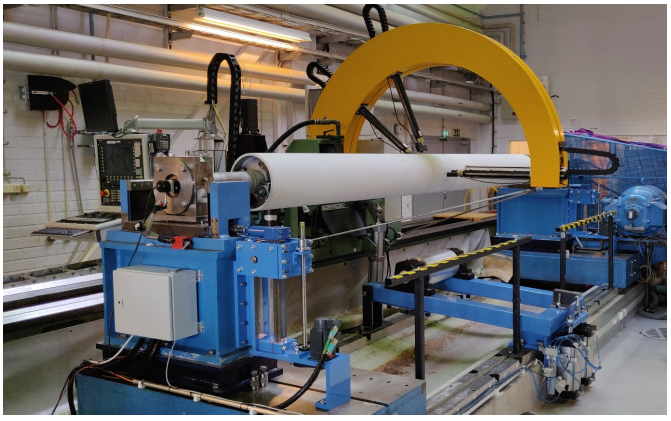

Fig. 4. The reflective laser sensors are attached to the yellow arc in the test setup

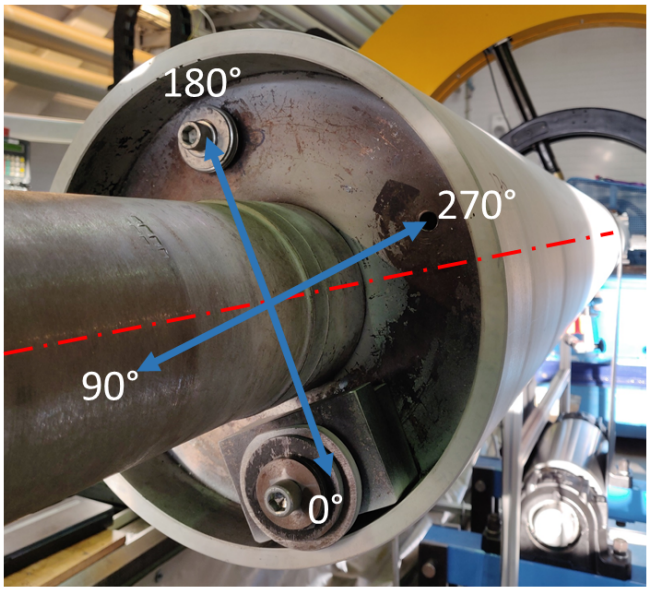

Fig. 5. The unbalance masses and the balancing masses attached to the Non-Drive End (NDE) end of the tube section

method, conducted with contactless laser displacement sensors. Sensor angles were 0°, 38° and 67° which minimized harmonic suppression assuming that rotor cross-section included less than 36 lobes [39]. The method separates the roundness profile from the center point movement, and thus the pure center point movement can be acquired. 100 rounds were measured including 1024 data points per revolution. With this sampling resolution, the sampling frequency increases over 16 kHz when using a 16 Hz rotation speed. Since the measured frequencies are low (1st critical speed = 21 Hz) the sampling frequency is considered reasonable and sufficient. The data acquisition was triggered with an encoder which ensured the measurements from the same phase. The encoder triggered signal enabled the use of time-synchronous averaging (TSA) method [40] that can be applied to similar phase-locked signals to represent an unaveraged large data set as an averaged one round data set. The center point movement could be presented as a resultant or its components in horizontal and vertical direction.

Table 1
Balancing masses used for initial balancing of the guiding roll for the paper machine

	Non-drive end of the rotor				Driving end of the rotor			
Phase [degrees]	0	90	180	270	0	90	180	270
Balancing mass [g]	2883	1056	159	0	2592	499	0	292

2.2.2. Simulation model

The rotor is modeled using the Timoshenko beam element [41] with two translational and two rotational degrees of freedom (DOF) at each node (Fig. 6). The bearings are formulated as linearized force coefficients (into stiffness and damping matrices of the system). The support is highly anisotropic with considerably higher stiffness in vertical direction than in the horizontal direction. Since in this test rotor, there is almost no cross-coupling between supports, a concentrated parameter approach is utilized by simplifying the support into horizontal and vertical spring-mass-damper elements [42,43]. The corresponding stiffness values in the horizontal and vertical directions are 18 MN/m and 200 MN/m, respectively. The rotor is supported with a pair of spherical roller bearings which were modeled based on kinematics and Hertzian contact theory [44]. The bearings are linearized at equilibrium condition and the stiffness is calculated.

The model is validated with free-free frequencies and supported frequencies measured from the actual machine, i.e. 75 Hz for free-free rotor, and supported frequencies of 20.9 Hz in horizontal direction and 30 Hz in vertical direction. The planes at nodes 6 and 20 are highlighted as the displacement are measured at these locations.

2.3. Validation with added unbalance

In order to validate the identified residuals, a known additional mass is added both at node 20 in the simulation model as well as the corresponding location in the experimental rotor. Next the simulated signal at nodes 6 and 20 are compared with these nodes to validate the remaining residual unbalance determined in single plane and two planes as explained in Sections 2.1.1 and 2.1.2. Table 2 shows the three different added masses used for the validation.

Table 2
Added unbalance masses in the non-drive end (node 20) and their phases for validation

Parameters	Case 1	Case 2	Case 3
Unbalance mass [g]	100	300	500
Phase [degrees]	90	180	270

3. RESULTS

This section presents the estimation of the residual unbalance in a single plane in the best possible location, random two planes and balancing planes respectively. To obtain preliminary results for this study, measured displacement signals are obtained from the end planes of the tubular section, as they are closest measurement locations to the bearings. In the numerical model in Fig. 5, these locations are at node 6 (measurement plane 1) and node 20 (measurement plane 2). The algorithm is designed to

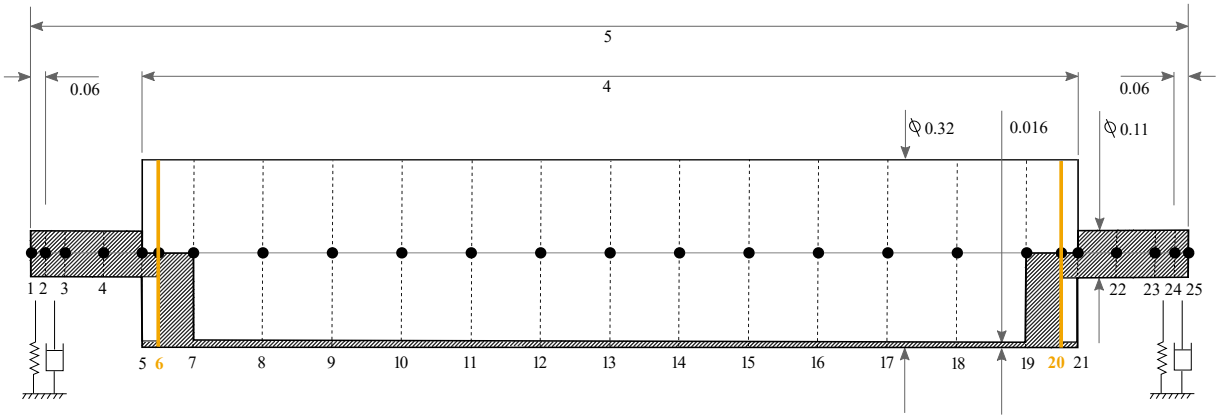

Fig. 6. Finite element discretized sketch of the rotor with key dimensions in meter [45]. Nodes 6 and 20 are the balancing planes as well as measurement plane for this study

calculate the residual with response signals from any single direction. In this case, only horizontal displacements were used from measurements as well as the model.

Since unbalance affects only the 1X harmonic component of the response, the measured signals are filtered using Fast Fourier transform (FFT). Figure 7 shows an example of how the 1X signal is isolated and the time domain signal is recreated using the 1X magnitude and phase for the next steps.

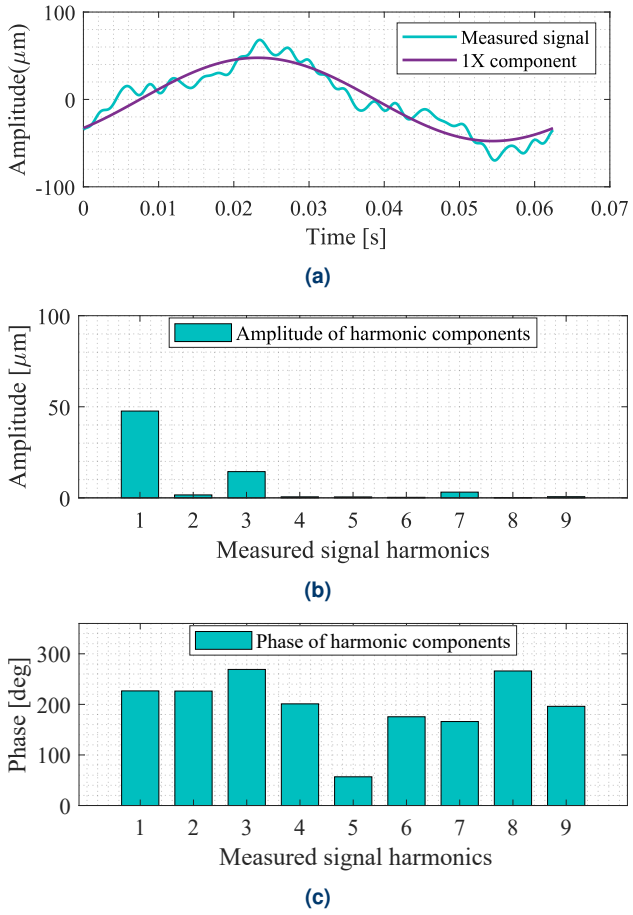

Fig. 7. An example of 1X component extraction from the measured signal at node 6 using FFT (a) The measured signal and the isolated 1X component (b) Amplitude and (c) Phase of components

3.1. Residual unbalance at single plane

Figure 8 graphically explains the numerical iteration process for identifying the magnitude and location of unbalance. For each node, a range of unbalance (0.001–0.1 kgm at an increment of 0.001) is selected. For this range, the displacement obtained from the model at node 6 (blue arrays of circles in Fig. 8a) is compared to measured amplitude (the red plane), and the intersection points are noted. Similarly, Fig. 8b is for node 20, where each point on the green line represents the displacements from the model which are compared to measured amplitude (yellow plane) and the intersection are noted. The intersection points from both figures are compared and only a single point emerges which most closely satisfies both the measured amplitudes at nodes 6 and 20.

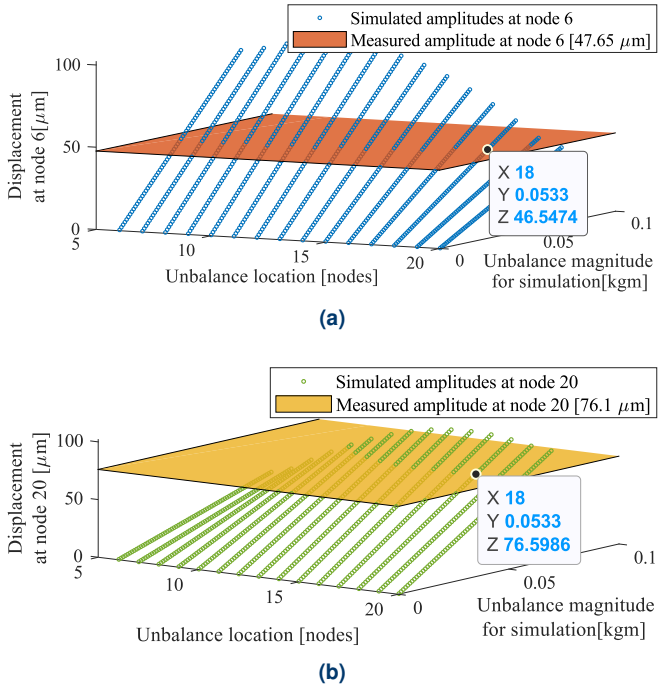

Fig. 8. Iterative matching of horizontal displacements at (a) node 6 and (b) node 20 (simulated vs measured) for single plane unbalance estimation. For each combination of unbalance magnitude (kgm) and the location (node), a simulated displacement is obtained. Only a single combination of unbalance magnitude (0.0533 kgm) and location (node 18) is achieved where the simulated displacements for both nodes (6, 20) match the measured amplitude

Once the unbalance magnitude and location are identified, the next step is phase correction by iteration. Iterating over a 0–360 degree range, the unbalance phase value is obtained which matches the measured signals both at node 6 and node 20 simultaneously as shown in Fig. 9.

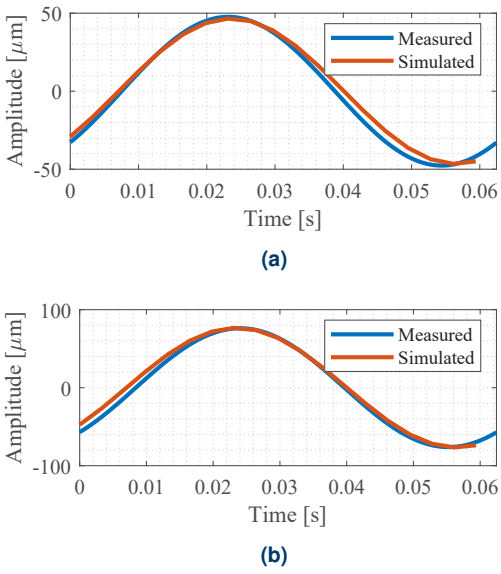

Fig. 9. Measured vs simulated signals at (a) Node 6 and (b) Node 20 for estimated resultant residual unbalance at a single plane (node 18)

Table 3
Best match residual unbalance parameters estimated in a single random plane

Best match unbalance parameters			Simulated amplitude [µm] (phase [°])		Measured amplitude [µm] (phase [°])		Error (%)	
Location [node]	Mag [kgm]	Phase [°]	Node 6	Node 20	Node 6	Node 20	Node 6	Node 20
18	0.0533	310	46.61 (217.4)	76.67 (217.9)	47.65 (226.6)	76.10 (221.6)	2.20 (4.0)	0.74 (1.6)

The final identified unbalance parameters: location, magnitude and phase for a single plane estimation of the residual unbalance is shown in Table 3. The error between the measured displacement amplitudes and the simulated displacement amplitudes in the measurement planes is also noted in the table.

3.2. Residual unbalance at two planes (random)

In this section, the residual unbalance is identified at two random planes that leads to the best match of the displacement from the model when compared to the measured signals at node 6 and 20. The overall process is similar to the single plane approach (Section 3.1) with one key difference. Here, for finding two planes, the iteration is divided into two parts: the first part from one end of the tube part of the rotor to the centre plane (node 6 to 13) and the second part for the rest of the remaining tube section (node 14 to 20). For these two sections, iteration for the location, magnitude and the phase difference between the two residuals are carried out.

Using the approach graphically explained in 8, the locations and the magnitudes of the two residuals are identified for the best match of amplitude between measured and simulated signal at node 6 and 20. Note that in the two planes case, the phase difference between the two residuals is identified in the same iteration as the location and the unbalance magnitude. However, depending upon how the two residuals are oriented with respect to the phase reference of the rotor, the measurement and simulated signals both at nodes 6 and 20 might still be out of phase. This is corrected by iterating the overall reference phase for 0–360 degree range, while keeping the phase difference between the two residuals fixed.

Figure 10 shows the simulated signal overlapping the measured signal quite well after magnitude and phase iteration for the estimated location of nodes 11 and 19 for the two residuals. The best matching unbalance parameters and their corresponding final simulated vs measurement comparison is shown in Table 4.

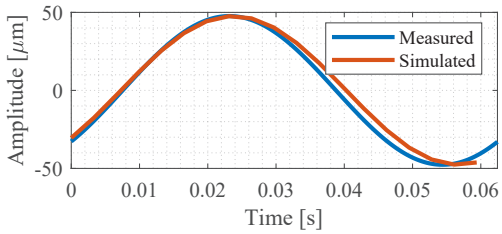

(a)

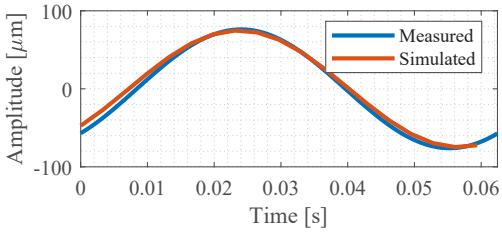

(b)

Fig. 10. Measured vs simulated signals at (a) Node 6 and (b) Node 20 for estimated resultant residual unbalance at two planes (nodes 11 and 19)

3.3. Residual unbalance at two balancing planes and validation

The previous sections were able to identify the location and parameters of the residual unbalance that best represent the state of the rotor as they were selected at random with the goal of optimization only. Those parameters have a usage in modeling and other goals, but for balancing purposes, those locations might not be directly useful due to design and accessibility-related limitations. For example, the identified residual unbalance planes (18 in single plane and 11 and 19 in double plane) are inappropriate for adding correction masses for the paper machine roll due to its design and application.

Table 4
Best match residual unbalance parameters estimated in two random planes

Best match unbalance parameters			Simulated amplitude [µm] (phase [°])		Measured amplitude [µm] (phase [°])		Error (%)	
Location [node]	Mag [kgm]	Phase [°]	Node 6	Node 20	Node 6	Node 20	Node 6	Node 20
11	0.010	310	47.52 (224.4)	74.63 (226.2)	47.65 (226.6)	76.10 (221.6)	0.27 (0.7)	1.93 (2.0)
19	0.045	320						

To solve this issue, the residuals can be identified directly at the balancing planes that are predetermined based on practical convenience. For the test rotor, the balancing planes are at nodes 6 and 20 as they have the proper attachment for adding correction masses (see Fig. 5). This way, in case the residual is higher than the defined limit, the balancing masses can be directly added in the same plane at the correct phase.

In the next two sections, first the residual unbalance is identified in the two balancing planes and then the results are validated using known unbalance masses in the model and the test rig.

3.3.1. Residual unbalance at two balancing planes

The residual unbalance estimation is similar to the two plane approach discussed in Section 3.2 One major difference is that the residual unbalance location is prefixed now (at nodes 6 and 20) and is not required to be estimated. Therefore, in this case, only the mass and phase have to be iterated and estimated. Figure 11 shows the best match between the measured and simulated signals at nodes 6 and 20 while Table 5 shows the estimated parameters.

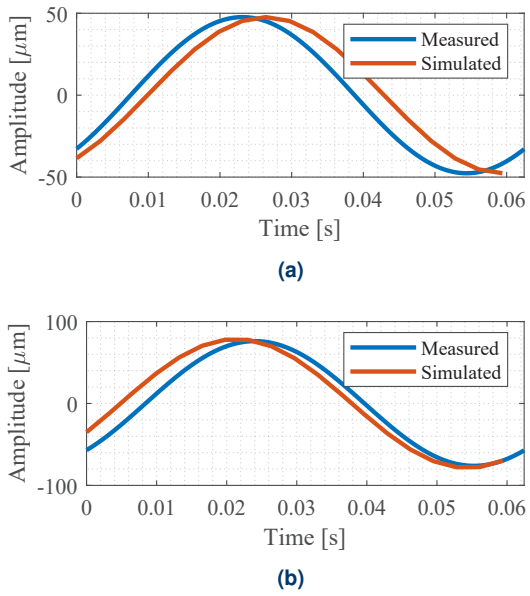

Fig. 11. measured vs simulated signals at (a) Node 6 and (b) Node 20 for estimated resultant residual unbalance at the balancing planes (nodes 6 and 20)

3.3.2. Robustness and sensitivity of estimation

For a model-based approach, it is important to test the sensitivity of the model against measurement and modeling errors through numerical analysis. Measurement noise might be there in the experimental data or the rotor model can often have missing or incorrect information which might lead to error in the simulated response. Therefore, for the identified unbalance parameters in two planes, first a modeling error is introduced and the change in the system response is observed in Table 6. The parameter varied is a localized mass of two elements at the drive end of the tube section of the rotor. The algorithm seems quite moderately sensitive to mass. However, it should be noted that the FE model-based algorithms are inherently highly sensitive to stiffness values as those are numerically large.

Although the model is verified with experimentally measured data, the data obtained here is extremely well processed which is not the case in general applications. Therefore, Table 6 also simulates the effect of measurement noise and its effect on the response comparison. The results in Table 6 shows that preprocessing through FFT is sufficient to eliminate most of the potential errors due to the Gaussian additive noise. Furthermore, since the balancing was not being performed in the case, a numerical validation of the method is carried out. In the simulation model, the correction masses of the same magnitude and opposite phase as the unbalance shown in Table 6 are added to different locations along the length of the rotor. Figure 12 shows that the displacements decrease significantly as the cor-

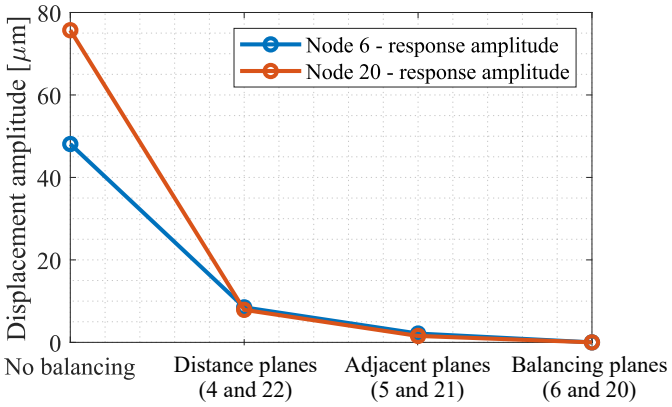

Fig. 12. Decrease in displacements as the correction mass is added in locations closer to the actual balancing planes where the unbalances were identified in Section 3.3.1

Table 5
Best match residual unbalance parameters estimated in two balancing planes (nodes 6 and 20)

Best match unbalance parameters			Simulated amplitude [μm] (phase [°])		Measured amplitude [μm] (phase [°])		Error (%)	
Location [node]	Mag [kgm]	Phase [°]	Node 6	Node 20	Node 6	Node 20	Node 6	Node 20
6	0.0110	306	48.09 (221.7)	75.74 (224.7)	47.65 (226.5)	76.10 (221.6)	0.92 (2.1)	0.47 (1.3)
20	0.0505	318						

Table 6
Sensitivity analysis of the response due to modeling and measurement error

	Simulated amplitude [μm] (phase [°])		Measured amplitude [μm] (phase [°])		Error (%)	
modeling error (%)	Node 6	Node 20	Node 6	Node 20	Node 6	Node 20
5	47.95 (224.7)	75.74 (221.6)	47.65 (226.5)	76.10 (221.6)	0.63 (2.16)	0.68 (1.40)
15	43.41 (224.9)	71.33 (224.9)	47.65 (226.5)	76.10(221.6)	8.90 (2.12)	6.27 (1.49)
25	40.71 (225.0)	68.78 (225.0)	47.65 (226.5)	76.10 (221.6)	14.56(2.12)	9.62 (1.53)
Measurement error (%)	Node 6	Node 20	Node 6	Node 20	Node 6	Node 20
5	48.09 (224.7)	75.74 (221.6)	47.71 (226.6)	76.11 (221.5)	0.80 (2.16)	0.49 (1.44)
15	48.09 (224.7)	75.74 (221.6)	47.25 (226.4)	75.99(221.6)	1.78 (2.08)	0.33(1.40)
25	48.09 (224.7)	75.74 (221.6)	46.94 (226.3)	76.71 (221.2)	2.45 (2.03)	1.26 (1.58)

rection mass is added in locations closer to the actual balancing planes where the unbalances were identified. This demonstrates that the estimated unbalance in balancing planes as shown in Table 6 is quite accurate and the post balancing vibration level is sensitive to the plane where the correction masses are added.

3.3.3. Validation of estimated residual (in balancing planes)

In this section, the residual unbalance in the two balancing planes (nodes 6 and 20) are integrated into the model. Along with that, a known unbalance mass is added to the model as well as the experimental setup and then the displacements from the model and the measurement (at the measurement planes) are compared. For the test case, three test cases are run with different masses (100 g, 300 g and 500 g) added at 90 degrees phase increment. The resulting comparison of simulated and measured signals (for added unbalance and initial residuals) is shown in Table 7.

4. DISCUSSION

The residual unbalance estimation for a single plane, two random planes and two balancing planes with the iterative method provided good estimation for the amount and phase of residual unbalance. The fact that the single-plane unbalance is identified at node 18 (0.0533 kgm) and the two plane estimation also have the higher residual around that location (node 19, 0.045 kgm) suggest that much of the randomly distributed residual unbalance in on the non-drive end (NDE) of the rotor bearing system. The residual estimation might be even better if the thickness variation along the rotor would be considered (in this study, it was simplified and studied as a symmetric tubular rotor). Another source of error includes the effect of bearing clearance which is not modelled in the linearized stiffness calculations for bearing. The actual bearing clearance, as the nominal clearance (60 μm) was used, combined with the extensive looseness in horizontal support might lead to nonlinear behaviour in the system response which is unaccounted in the simulation model.

Lastly, the validation of the estimated residual also suggests that the higher amount of residuals are distributed in the NDE side. For the 100 g additional mass with a previous residual of 0.057 kgm, there is no significant change in the amplitude of vibration in Table 7 for both measured and simulation. For the 300 g added at 180 deg, and with the residual 0.057 kgm at 310 deg, the vibration does not increase much in the simulation as the relative phase of the two masses are quite opposite while in measured data trend the amplitude is increasing rapidly. Figure 13 depicts the added mass relation to residual unbalance in the studied four cases. The resultant unbalance mass and direction are depicted. Figure 14 depicts the thickness profile of the roll cross-section measured in an earlier study [46]. This difference leads to a large error in the comparison between measured and simulated for the 300 g case. For the 500 g added mass at 270 deg, both of the large masses at node 20 are quite close to each other and pull in unison which leads to an increase in the displacement amplitude for both simulated and measured data.

Table 7
Validation of initial residual by comparing displacement amplitudes with three added mass cases

Added mass [g]	Simulated amplitude [μm] (phase [°])		Measured amplitude [μm] (phase [°])		Error (%)	
	Node 6	Node 20	Node 6	Node 20	Node 6	Node 20
0	48.09 (221.7)	75.74 (224.7)	47.65 (226.5)	76.10 (221.6)	0.92 (2.1)	0.47 (1.3)
100	43.28 (214.8)	65.99 (215.6)	37.10 (211.1)	65.63 (208.3)	16.65 (1.7)	0.06 (3.5)
300	52.08 (195.6)	67.96 (188.1)	78.49 (201.0)	140.61 (200.1)	34.92 (2.6)	51.67 (5.9)
500	78.57 (241.3)	141.10 (246.3)	89.52 (248.7)	145.56 (249.7)	12.52 (2.9)	3.04 (1.3)

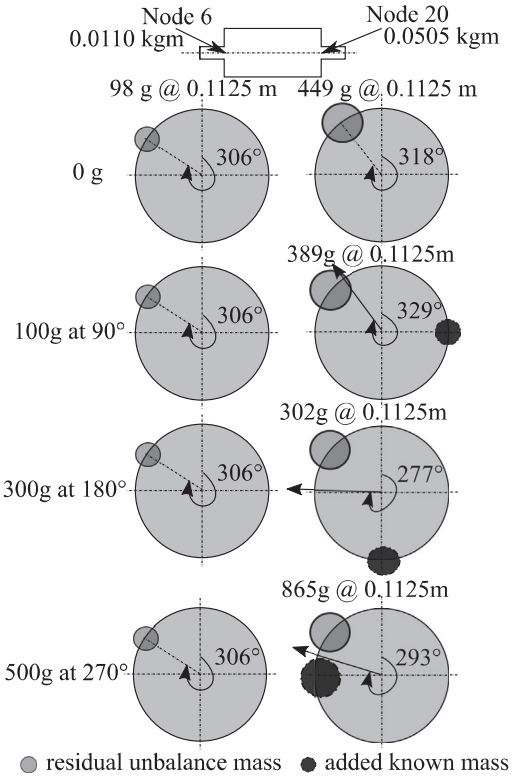

Fig. 13. Added unbalances and phases in the 0 g, 100 g, 300 g and 500 g cases

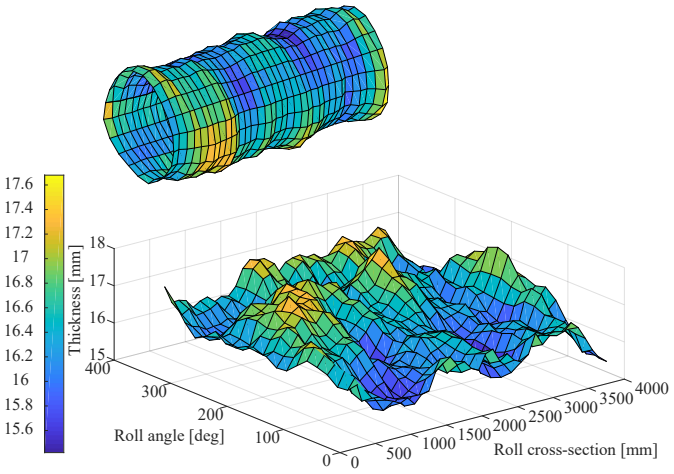

Fig. 14. Measured thickness profile of the actual rotor

5. CONCLUSION

A method for identification of residual unbalance was developed during the research. The method can be used as a post-balancing quality check for onsite rotors at service speed. For example, the digital twins, where the actual physical twin is replicated with physics-based simulation, require high accuracy model as a basis to assess the state of the rotating machine, thus the identification of residual unbalance is of importance. The results were validated with an industrial scale case study. In the study the absolute displacement of the rotor was used. High accuracy was obtained when two measurements were used in the horizontal direction.

The method creates a foundation for other, more common signals, e.g., accelerometer and force measurements at bearing locations to be used for unbalance estimation. Such sensors are more prevalent across industries and would make the proposed solution for balancing quality check more practical and widely applicable. The iterative method allows us to include the dynamic model to the algorithm, and therefore can account for the dynamic behavior more accurately when compared to an intelligent algorithm based purely on heuristic data. However, in future research, the proposed method can be combined with intelligent algorithms for further optimizing the computational efficiency. For example, neural networks can utilize vibration data from the finite element model for training and predicting initial residual unbalance in an actual machine.

ACKNOWLEDGEMENTS

The research is funded by Business Finland project BRAIN (decision no. 1119/31/2018).

REFERENCES

[1] A. Shrivastava and A.R. Mohanty, "Estimation of single plane unbalance parameters of a rotor-bearing system using kalman filtering based force estimation technique," *J. Sound Vib.*, vol. 418, pp. 184–199, 2018, doi: 10.1016/j.jsv.2017.11.020.

[2] E. Thearle, "Dynamic balancing of rotating machinery in the field," *Trans. ASME*, vol. 56, no. 10, pp. 745–753, 1934.

[3] K. Hopkirk, "Notes on methods of balancing," *The engineer*, vol. 170, pp. 38–39, 1940.

[4] S. Zhou, S.W. Dyer, K.-K. Shin, J. Shi, and J. Ni, "Extended Influence Coefficient Method for Rotor Active Balancing During Acceleration," *J. Dyn. Syst. Meas. Contr.*, vol. 126, no. 1, pp. 219–223, 04 2004, doi: 10.1115/1.1651533.

[5] T.P. Goodman, "A Least-Squares Method for Computing Balance Corrections," *J. Eng. Ind.*, vol. 86, no. 3, pp. 273–277, 08 1964, doi: 10.1115/1.3670532.

[6] M.S. Darlow, "Balancing of high-speed machinery: Theory, methods and experimental results," *Mech. Syst. Sig. Process.*, vol. 1, no. 1, pp. 105–134, 1987, doi: 10.1016/0888-3270(87)90087-2.

[7] E. Gunter *et al.*, "Balancing of multimass flexible rotors," in *Proceedings of the 5th Turbomachinery Symposium*. Texas A&M University. Gas Turbine Laboratories, 1976, doi: 10.21423/R1W38D.

[8] R.E.D. Bishop and G.M.L. Gladwell, "The vibration and balancing of an unbalanced flexible rotor," *J. Mech. Eng. Sci.*, vol. 1, no. 1, pp. 66–77, 1959, doi: 10.1243/JMES_JOUR_1959_001_010_02.

[9] R.E.D. Bishop, "On the possibility of balancing rotating flexible shafts," *J. Mech. Eng. Sci.*, vol. 24, no. 4, pp. 215–220, 1982, doi: 10.1243/JMES_JOUR_1982_024_040_02.

[10] J.W. Lund and J. Tonnesen, "Analysis and experiments on multiplane balancing of a flexible rotor," *J. Eng. Ind.*, vol. 94, no. 1, pp. 233–242, 1972, doi: 10.1115/1.3428116.

[11] M.S. Darlow, Review of Literature on Rotor Balancing. New York, NY: Springer New York, 1989, pp. 39–52, doi: 10.1007/978-1-4612-3656-6_3.

[12] ISO, "Mechanical vibration. rotor balancing. part 11: Procedures and tolerances for rotors with rigid behaviour," International Organization for Standardization, Geneva, CH, Standard ISO 21940–11:2016, 2016. [Online]. Available: https://www.iso.org/standard/54074.html.

[13] R. Platz and R. Markert, "Fault models for online identification of malfunctions in rotor systems," *Transactions of the 4th International Conference Acoustical and Vibratory Surveillance, Methods and Diagnostic Techniques, University of Compiegne, France*, vol. 2, pp. 435–446., 2001.

[14] R. Markert, R. Platz, and M. Seidler, "Model based fault identification in rotor systems by least squares fitting," *Int. J. Rotating Mach.*, vol. 7, no. 5, pp. 311–321, 2001.

[15] J.R. Jain and T.K. Kundra, "Model based online diagnosis of unbalance and transverse fatigue crack in rotor systems," *Mech. Res. Commun.*, vol. 31, no. 5, pp. 557–568, 2004.

[16] G.N.D.S. Sudhakar and A.S. Sekhar, "Identification of unbalance in a rotor bearing system," *J. Sound Vib.*, vol. 330, no. 10, pp. 2299–2313, 2011.

[17] J. Yao, L. Liu, F. Yang, F. Scarpa, and J. Gao, "Identification and optimization of unbalance parameters in rotor-bearing systems," *J. Sound Vib.*, vol. 431, pp. 54–69, 2018.

[18] N. Bachschmid, P. Pennacchi, and A. Vania, "Identification of multiple faults in rotor systems," *J. Sound Vib.*, vol. 254, no. 2, pp. 327–366, 2002.

[19] P. Pennacchi, R. Ferraro, S. Chatterton, and D. Checcacci, "A model-based prediction of balancing behavior of rotors above the speed range in available balancing systems," in *Turbo Expo: Power for Land, Sea, and Air*, vol. 10 B. Virtual, Online: American Society of Mechanical Engineers, September, 2020, p. V10BT29A015.

[20] P. Pennacchi, "Robust estimation of excitations in mechanical systems using m-estimators – experimental applications," *J. Sound Vib.*, vol. 319, no. 1–2, pp. 140–162, 2009.

[21] D. Zou, H. Zhao, G. Liu, N. Ta, and Z. Rao, "Application of augmented Kalman filter to identify unbalance load of rotor-bearing system: Theory and experiment," *J. Sound Vib.*, vol. 463, p. 114972, 2019.

[22] O. Mey, W. Neudeck, A. Schneider, and O. Enge-Rosenblatt, "Machine learning-based unbalance detection of a rotating shaft using vibration data," in *25th IEEE International Conference on Emerging Technologies and Factory Automation*, Vienna, Austria, September, 2020, pp. 1610–1617.

[23] G. Hübner, H. Pinheiro, C. de Souza, C. Franchi, L. da Rosa, and J. Dias, "Detection of mass imbalance in the rotor of wind turbines using support vector machine," *Renewable Energy*, vol. 170, pp. 49–59, 2021, doi: 10.1016/j.renene.2021.01.080.

[24] A.A. Pinheiro, I.M. Brandao, and C. Da Costa, "Vibration analysis in turbomachines using machine learning techniques," *Eur. J. Eng. Technol. Res.*, vol. 4, no. 2, pp. 12–16, 2019.

[25] J.K. Sinha, A. Lees, and M. Friswell, "Estimating unbalance and misalignment of a flexible rotating machine from a single rundown," *J. Sound Vib.*, vol. 272, no. 3–5, pp. 967–989, 2004.

[26] J. Sinha, M. Friswell, and A. Lees, "The identification of the unbalance and the foundation model of a flexible rotating machine from a single run-down," *Mech. Syst. Sig. Process.*, vol. 16, no. 2, pp. 255–271, 2002, doi: 10.1006/mssp.2001.1387.

[27] S. Edwards, A. Lees, and M. Friswell, "Experimental identification of excitation and support parameters of a flexible rotor-bearings- foundation system from a single run-down," *J. Sound Vib.*, vol. 232, no. 5, pp. 963–992, 2000.

[28] A. Lees, J.K. Sinha, and M. Friswell, "The identification of the unbalance of a flexible rotating machine from a single rundown," *J. Eng. Gas Turbines Power*, vol. 126, no. 2, pp. 416–421, 2004.

[29] A. Lees, J.K. Sinha, and M.I. Friswell, "Estimating rotor unbalance and misalignment from a single run-down," in *Mater. Sci. Forum*, vol. 440. Trans Tech Publ, 2003, pp. 229–236.

[30] S.M. Ibn Shamsah and J.K. Sinha, "Rotor unbalance estimation with reduced number of sensors," *Machines*, vol. 4, no. 4, p. 19, 2016.

[31] S.I. Shamsah, J. Sinha, and P. Mandal, "Application of modelbased rotor unbalance estimation using reduced sensors and data from a single run-up," in *2nd International Conference on Maintenance Engineering (IncoME-II)*, 2017.

[32] S.M.I. Shamsah, J.K. Sinha, and P. Mandal, "Estimating rotor unbalance from a single run-up and using reduced sensors," *Measurement*, vol. 136, pp. 11–24, 2019.

[33] E. Knopf, T. Krüger, and R. Nordmann, "Residual unbalance determination for flexible rotors at operational speed," in *Proceedings of the 9th IFToMM International Conference on Rotor Dynamics*, P. Pennacchi, Ed. Cham: Springer International Publishing, 2015, pp. 757–768, doi: 10.1007/978-3-319-06590-8_62.

[34] Y. Khulief, M. Mohiuddin, and M. El-Gebeily, "A new method for field-balancing of high-speed flexible rotors without trial weights," *Int. J. Rotating Mach.*, vol. 2014, 2014, doi: 10.1155/2014/603241.

[35] R. Nordmann, E. Knopf, and B. Abrate, "Numerical analysis of influence coefficients for on-site balancing of flexible rotors," in *Proceedings of the 10th International Conference on Rotor Dynamics – IFToMM*, K.L. Cavalca and H.I. Weber, Eds. Cham: Springer International Publishing, 2019, pp. 157–172, doi: 10.1007/978-3-319-99272-3_12.

[36] ISO, "Mechanical vibration. rotor balancing. part 12: Procedures and tolerances for rotors with flexible behavior," International Organization for Standardization, Geneva, CH, Standard ISO 21940-12, 2016, https://www.iso.org/standard/50429.html.

[37] M.I. Friswell, J.E. Penny, A.W. Lees, and S.D. Garvey, *Dynamics of rotating machines*. Cambridge University Press, 2010.

[38] P. Kuosmanen and P. Väänänen, "New highly advanced roll measurement technology," in *Proc. 5th International Conference on New Available Techniques, The World Pulp and Paper Week*, 1996, pp. 1056–1063.

[39] H. Kato, R. Sone, and Y. Nomura, "In-situ measuring system of circularity using an industrial robot and a piezoactuator," *Int. J. Jpn. Soc. Precis. Eng.*, vol. 25, no. 2, pp. 130–135, 1991.

[40] P. McFadden, "A revised model for the extraction of periodic waveforms by time domain averaging," *Mech. Syst. Sig. Process.*, vol. 1, no. 1, pp. 83–95, 1987, doi: 10.1016/0888-3270(87)90085-9.

[41] H.D. Nelson, "A Finite Rotating Shaft Element Using Timoshenko Beam Theory," *J. Mech. Des.*, vol. 102, no. 4, pp. 793–803, 10 1980, doi: 10.1115/1.3254824.

[42] K. Cavalca, P. Cavalcante, and E. Okabe, "An investigation on the influence of the supporting structure on the dynamics of the rotor system," *Mech. Syst. Sig. Process.*, vol. 19, no. 1, pp. 157–174, 2005, doi: 10.1016/j.ymssp.2004.04.001.

[43] P.F. Cavalcante and K. Cavalca, "A method to analyse the interaction between rotor-foundation systems," in *SPIE proceedings series*, 1998, pp. 775–781.

[44] B. Ghalamchi, J. Sopanen, and A. Mikkola, "Modeling and dynamic analysis of spherical roller bearing with localized defects: analytical formulation to calculate defect depth and stiffness," *Shock Vib.*, vol. 2016, 2016, doi: 10.1155/2016/2106810.

[45] T. Choudhury, R. Viitala, E. Kurvinen, R. Viitala, and J. Sopanen, "Unbalance estimation for a large flexible rotor using force and displacement minimization," *Machines*, vol. 8, no. 3, 2020, doi: 10.3390/machines8030039.

[46] J. Juhanko, E. Porkka, T. Widmaier, and P. Kuosmanen, "Dynamic geometry of a rotating cylinder with shell thickness variation," *Est. J. Eng.*, vol. 16, no. 4, p. 285, 2010.